Research Article

Hongcai Li[#], Qian Wu[#], Xiaofei Yuan, Yonggang Li, Ying Xu*, and Ruoyu Hong*

Preparation of water-based dextran-coated Fe_3O_4 magnetic fluid for magnetic hyperthermia

https://doi.org/10.1515/ntrev-2022-0534
received March 22, 2022; accepted March 15, 2023

Abstract: Fe_3O_4 nanoparticles were prepared by chemical co-precipitation, modified with dextran, and dispersed in water to form a magnetic fluid (MF) for use in biomedical areas. The analyses of stability and magnetic property demonstrate that the prepared functional MF possesses outstanding stability (stability index within 60 days, high dilution stability, and autoclaved stability) and high magnetization (the values χ and M_s of MF are 5.87×10^{-4} and 20.57 emu/g, respectively). Due to the coating of dextran, the toxicity of MF is minimal (*in vitro* survival rate of MCF-7 cells, blood compatibility, and *in vivo* toxicity). In addition, although the outer layer is coated with dextran, the M_s intensity remains high, so the Fe_3O_4 MF owns a fast magnetic temperature response (when the MF concentration is 55 mg/mL, it can rapidly rise to 55°C within 800 s), which plays an extremely vital role in MF hyperthermia. So, the MF can effectively cause necrosis of human lung A549 cells, which shows a certain application potential.

Keywords: magnetic fluid, biocompatibility, magnetic hyperthermia

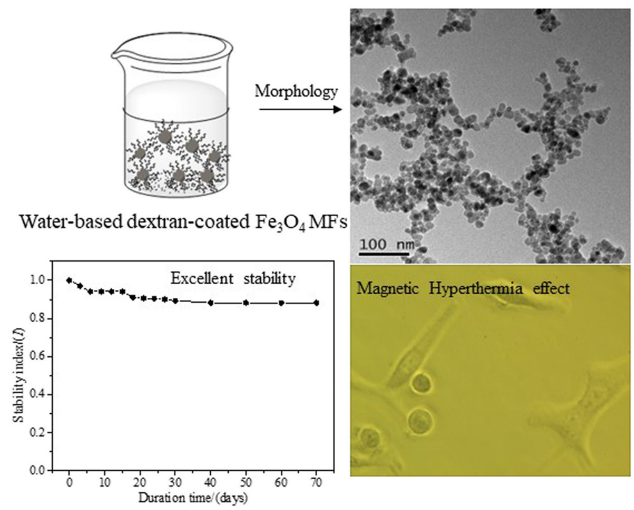

Graphical abstract

1 Introduction

Magnetic fluid (MF), colloidal suspension, consists of nanoparticles with the size of 1–100 nm [1]. Water, silicone oil, kerosene, and ethanol/water mixture can be used as the carrier liquid for MF [2]. But water-soluble MF is more inclined to biological applications [3]. Due to the large density difference of nanoparticles in the carrier liquid, the MF exhibits weak stability under gravity, centrifugal force, and magnetic force [4]. Nanoparticles have unique properties such as “small size effect,” “surface effect,” “quantum tunnel effect,” *etc.* [5]. Therefore, the MF exhibits many unique properties attracting more and more researchers [6].

One of the most peculiar properties of nanoparticles in the MF is superparamagnetism [7], which can be utilized commendably. In addition, the MF possesses both magnetism and fluidity [8]. Therefore, many peculiar functions can be seen, which undoubtedly show tremendous application potential in diverse areas [9], for example, biomedicine including diagnostics, targeting drug delivery systems, biosensors, magnetic cell separation and purification, enzyme and protein immobilization, magnetic resonance imaging, MF hyperthermia, and many other

# These authors contributed equally to this work and should be considered first co-authors.

* **Corresponding author: Ying Xu,** College of Chemical Engineering, Fuzhou University, Fuzhou, Fujian 350108, China, e-mail: xuying31@fzu.edu.cn
* **Corresponding author: Ruoyu Hong,** College of Chemical Engineering, Fuzhou University, Fuzhou, Fujian 350108, China, e-mail: rhong@fzu.edu.cn
Hongcai Li, Qian Wu, Xiaofei Yuan: College of Chemical Engineering, Fuzhou University, Fuzhou, Fujian 350108, China
Yonggang Li: Radiological Department, The First Affiliated Hospital of Soochow University, Suzhou 215006, China

applications [10]. Among them, biological applications have become increasingly promising research areas [11]. Consequently, the preparation of stable and harmless MF must be taken into account [12]. While owing to the high surface energy of nanoparticles, it is a great challenge to prepare stable MF without aggregation [13].

To obtain well-dispersed MF, many researchers have made various attempts at nanoparticle modification [14]. Racuciu and Oancea [15] modified the magnetic nanoparticles with tetramethylammonium hydroxide (TMAH) to prevent magnetic nanoparticles from aggregation and keep magnetic nanoparticles well-dispersed in deionized water, which can be applied in many technological areas. Goharkhah *et al.* [16] also tailored monodisperse water-based MF capped by TMAH, which is of great significance for convective heat transfer. Huessein Mohd *et al.* [17] coupled the polyvinyl alcohol to the surface of magnetic nanoparticles successfully. Rahman and Ochiai [18] presented that magnetic nanoparticles were functionalized with chitosan and then reacted with butane tetracarboxylic dianhydride, exhibiting good dispersibility in aqueous media. Surfactants have vital effects on the properties of the MF, such as thermal conductivity [19], which indicates that the selection of the surfactant seems to be extremely significant in the relevant applications. High magnetite concentration and magnetization, as well as excellent stability, are expected in the applications of MF [20], the appropriate surfactants with long molecular chains can be adopted to prepare an ideal MF [21]. Dextran can yet be regarded as a superb surfactant in view of the fact that it possesses a great number of hydroxy groups, which can stabilize magnetic nanoparticles in water because of the strong chelation between Fe_3O_4 nanoparticles and hydroxy groups [22]. In addition, dextran shows excellent biocompatibility, so it shows a certain application potential [23]. Therefore, dextran-functionalized Fe_3O_4 MF is generally employed for bio-applications [23]. There are many similar applications, for example, Shaterabadia *et al.* [24] showed a detailed study of the hyperthermia effect produced by dextran-coated ferric tetroxide nanoparticles of different sizes. Similarly, Linh *et al.* [25] prepared dextran-coated Fe_3O_4 nanoparticles by coprecipitation method and applied them to the hyperthermia treatment of cancer. Naik *et al.* [26] further investigated in detail the factors influencing the generation of magneto-thermal effects, such as magnetic properties, temperature, and viscosity of the carrier liquid.

Although the effect of hyperthermia on dextran-coated Fe_3O_4 nanoparticles is significant in previous articles, excellent biocompatibility *in vivo* is also important, especially the safe dosage and whether it will cause an inflammatory reaction [27]. This is because excellent biocompatibility is one of the primary conditions in practical clinical application. Therefore, we take biocompatibility as one of the main research projects, and focus on the safe dosage range and determine whether it causes an inflammatory reaction, to ensure excellent biocompatibility.

In addition, excellent MF hyperthermia owns stable water-based MF with a fast magnetic temperature response [25]. So, we used the coprecipitation method to prepare dextran-coated Fe_3O_4 MF with excellent stability. The key to preparation is to add dextran several times, which contributes to dextran fully contacting and reacting with Fe_3O_4. In short, the particle size, magnetization, and stability, as well as the toxicity of the dextran-modified Fe_3O_4 MF, were characterized by transmission electron microscopic (TEM), a Gouy magnetic balance, and toxicological experiments, respectively. We focused on the stability, magnetic properties, biocompatibility *in vivo* and *in vitro*, and the effect of magnetic hyperthermia.

2 Experimental

2.1 Materials

All chemicals were analytical grade and used without further purification. Iron(III) chloride hexahydrate ($FeCl_3 \cdot 6H_2O$), iron(II) sulfate heptahydrate ($FeSO_4 \cdot 7H_2O$), ammonia solution (25 wt%), dextran with molecule weight of 20,000 (T20), and absolute ethyl alcohol were all purchased from Sinopharm Chemical Reagent Co. Ltd. Deionized water was used throughout the experiments.

2.2 Preparation of functional MF

The dextran-functionalized MF was prepared by the chemical co-precipitation method, and considering the influence of the molecular weight of dextran [28], dextran with a molecular weight of 20 kDa is selected as the outer layer. The specific preparation process is as follows. A mixed solution (30 mL) of iron(III) chloride hexahydrate (0.44 g, 1.6 mM) and iron(II) sulfate heptahydrate (0.22 g, 0.8 mM) with a molar ratio of 2:1 was added into 250 mL three-necked flash with slow stirring at the speed of 160 rpm/min for 10 min under argon protection at room temperature. The temperature was raised to 60°C, then 13 mL of ammonia solution was rapidly poured into the three-necked bottle with vigorous stirring (240 rpm/min) for 5 min, followed by relatively slow stirring (100 rpm/min).

The mixture became black immediately once the ammonia was added. After that, Dextran (8 g, 0.4 mM) was added to the black suspension in 5 equal portions and reacted in argon for 60 min. The heating was stopped and the black suspension was cooled to room temperature under slow stirring. Then, dextran-coated Fe_3O_4 magnetic nanoparticles were washed with absolute ethyl alcohol and deionized water mixed with the aqueous solution, and separated by a permanent magnet, repeating this process several times. Then, dextran-coated Fe_3O_4 magnetic nanoparticles were washed with deionized water like the above process until all ions were removed. The magnetic nanoparticles collected by magnetic separation were dispersed in deionized water by ultrasonic vibration with the addition of 1.2 g dextran followed by 30 min of ultrasound. Finally, the stable dextran-functional MF was successfully prepared.

2.3 Characterizations

Scanning electron microscopy (SEM) and TEM was performed using SU8010 ESEM Hitachi microscope (Hitachi, Japan) and a JEM 2100 F, JEOL, Japan, operating at 8.0 and 200 kV, respectively. X-ray diffraction (XRD) measurement was recorded on an X-ray diffractometer (R-AXIS RAPID-F Rigaku Corporation, Japan) using a Co target (λ = 1.5418 Å) at a generator voltage of 40 kV and current of 20 mA. Fourier transform infrared spectroscopy carried out on Thermo Nicolet 670 FTIR instrument (Thermo Nicolet Corporation, USA) was employed to evaluate the success of functionalization operating at the wavelength range of 4,000–400 cm^{-1}. The magnetization of the magnetic nanoparticles was obtained by a vibrating sample magnetometer (VSM-7400, Lake Shore, USA), and the magnetization of the functional MF was determined on a Gouy magnetic balance (CTP-II, Nanjing Sangli, China). Hydrodynamic diameter distribution was detected by the Malvern Laser Particle Size Analyzer (Mastersizer 3000, Malvern, Germany). The magnetic hyperthermia experiments of the dextran-coated Fe_3O_4 MF in the AC magnetic field were performed on a medium-frequency induction heating apparatus (Chien-Wah Co., Ltd, Dongguan, China).

2.4 Toxicological experiments

The MF must be nontoxic if it is applied for hyperthermia. So, it is essential to test the toxicity of MF, including the experiments *in vitro* and *in vivo*.

2.4.1 *In vitro*

The toxicity of the obtained MF *in vitro* was tested by the MTT method [29]. Human breast cancer cell MCF-7 cells were inoculated in a 96-well plate (200 µL). The MF with different Fe concentrations was added and cultivated for 24 h, then the cell viability was determined.

2.4.2 *In vivo*

The clean-grade Kunming mice, from the animal room of the Medical College of Soochow University, weighing 20–24 g and aged 6–8 weeks (with the experimental animal production license: SCXK (Su) 2008-0035), were housed in the experimental animal barrier system of the Experimental Animal Center of Soochow University. The air cleanliness was 10,000, the frequency of ventilation was 15 times/h, the temperature was 21–24°C, and the humidity was 75–80%. The laboratory animal use license is SYXK (Su) 2008-0113.

In the short-term distribution experiment, 60 healthy mice were divided into 4 groups, the control group, the low dose group, the middle dose group, and the high dose group based on the preliminary experiment. There were 15 mice in each group. The control group was given physiological saline.

The obtained Fe_3O_4 MF with the prescribed dose was injected into the mice by the caudal vein injection and the intraperitoneal injection method according to the standard mouse body weight. At 12, 24, and 36 h before and after the injection, blood was collected through an orbital vein, and the white cells of anticoagulant blood were measured by an automatic blood cell counter to observe the toxicity of the mice and the changes in subjective signs.

In the long-term distribution experiment, 40 healthy mice were also divided into four groups, which were set to be empty control group, the low-dose group, the middle-dose group, and the high-dose group. The mice with half male and female in each group were disposably injected at different doses through the tail vein and the intraperitoneal injection, and the acute poisoning performance and death of the mice were observed.

3 Results and discussion

3.1 Characterization of magnetic nanoparticles

SEM images in Figure 1a and b show the patterns of uncoated and dextran-coated Fe_3O_4 magnetic nanoparticles,

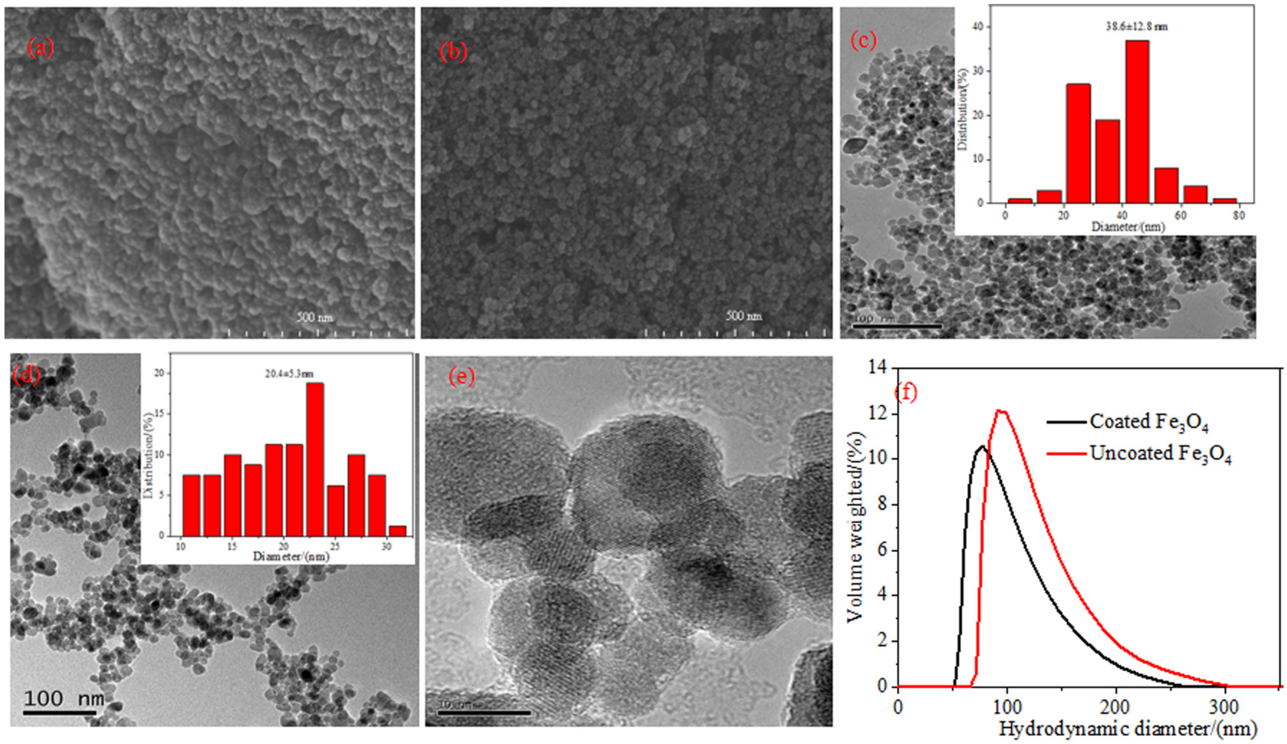

Figure 1: Morphology characterization of MFs: SEM of (a) uncoated Fe_3O_4 magnetic nanoparticles and (b) dextran-coated Fe_3O_4 magnetic nanoparticles, the scale bars are all 500 nm; TEM of (c) uncoated Fe_3O_4 magnetic nanoparticles and (d and e) dextran-coated Fe_3O_4 magnetic nanoparticles, the scale bars of (c) and (d) are 100 nm, and (e) are 10 nm; (f) hydrodynamic diameter distribution by DLS.

which look spherical and also present a certain stacking. TEM shown in Figure 1c–e is employed to observe the morphology of uncoated and dextran-coated Fe_3O_4 magnetic nanoparticles in MF. We can observe from Figure 1c and d that when coated with dextran, Fe_3O_4 nanoparticles can be considered roughly spherical. As exhibited in Figure 1c, uncoated magnetic nanoparticles in MF tend to aggregate because of high surface energy as well as large specific surfaces. The nanoparticles are connected, the dispersion of the particles is not good, and the average particle size reaches 38.6 nm. In a contrast, Figure 1d exhibits the dextran-coated Fe_3O_4 magnetic nanoparticles, which demonstrate superb monodispersity in MF, with scarcely any aggregation, and the average particle size is about 20.4 nm. This is attributed to the electrostatic and steric repulsion among the dextran-coated magnetic nanoparticles [30]. Figure 1e shows that a core-shell structure was formed between Fe_3O_4 magnetic nanoparticles and dextran, which certified that dextran had been successfully coated on the surface of Fe_3O_4 nanoparticles.

After diluting the prepared Fe_3O_4 MF by a certain factor (0.2 g/L), the hydrodynamic diameter distribution of the magnetic nanoparticles was measured by DLS. It can be seen from Figure 1f that both the uncoated and dextran-coated Fe_3O_4 MF are monodisperse, and the particle size distribution range is narrow. The average hydrodynamic diameter of the uncoated and dextran-coated particles is 118 nm (PDI = 0.19) and 97 nm (PDI = 0.13), respectively. It can be seen that the hydrodynamic diameter of bare Fe_3O_4 magnetic nanoparticles is larger than that of dextran-coated magnetic nanoparticles, which is due to the higher surface energy of uncoated magnetic nanoparticles, causing agglomeration among the nanoparticles [31]. The result is consistent with that of SEM and TEM.

Figure 2a is the XRD patterns of uncoated and dextran-coated Fe_3O_4 magnetic nanoparticles in MF, which investigates the crystalline phases. The characteristic diffraction peaks at 30.0, 35.5, 43.0, 53.0, 57.0, and 62.6° observed from the XRD patterns belonged to (220), (311), (400), (422), (511), and (440) planes of samples, respectively, which was consistent with the inverse cubic spinel phase of Fe_3O_4 (JCPDS card No. 75-1609) [32]. It can be seen from the XRD pattern of the dextran-coated Fe_3O_4 that the position of the major peaks does not change. That is to say, the crystal phase of the Fe_3O_4 nanoparticles does not change after being coated with dextran.

The size of Fe_3O_4 nanoparticles can be calculated according to the Scherrer formula: $D = K\lambda/(B\cos\theta)$ (where D is the average thickness perpendicular to the crystal plane direction, *K* is the Scherrer constant, *λ* is the X-ray wavelength, *B* is the half-width of the diffraction peak, and *θ* is the diffraction angle) [33]. The particle sizes before and after coating with dextran were 13.4 and 12.5 nm, respectively. More encouragingly, the size of the dextran-coated iron tetroxide did not increase but decreased accordingly, which indicates that there is a significant aggregation of the uncoated nanoparticles, and the aggregates are considered single crystals. Therefore, the particle size of the uncoated nanoparticles has a larger diameter calculated by the Scherrer formula. The change in size indirectly reflects the aggregation state between nanoparticles. Figure 2b illustrates the FTIR spectrum of dextran powder, uncoated Fe_3O_4 magnetic nanoparticles, and dextran-coated Fe_3O_4 magnetic nanoparticles. From the spectrum of uncoated magnetic nanoparticles in Figure 2b(I), it can be found that the characteristic absorption of the Fe–O bond appears at the peaks of around 550 cm^{-1}, which certifies the existence of magnetic nanoparticles [34]. The broad absorption peak at 3,318 cm^{-1} belongs to the hydroxyl group on the surface of magnetic nanoparticles, and the peak at 1,633 cm^{-1} is contributed to vibration absorption peaks of water molecules. As to the FTIR spectrum of dextran in Figure 2b(III), there are characteristic absorption peaks of C–O–C bonds at about 1,141 cm^{-1}. Due to the vibration absorption of C–H, H–C–OH, and $=CH_2$, there are peaks at 2,903, 1,640, and 1,415 cm^{-1} respectively [35]. As shown in Figure 2b(II), Fe_3O_4 magnetic nanoparticles have strong absorption peaks at 1,146 and 557 cm^{-1}, while the intensity of absorption peak at 2,903 cm^{-1} has dropped to a large extent because the hydrogen atoms on the surface of the dextran combine with the oxygen atoms on the surface of Fe_3O_4 nanoparticles [36]. Comparing Figure 2b(I–III), the spectrum of Fe_3O_4 magnetic nanoparticles coated by dextran exhibits the characteristic peaks of Fe_3O_4 magnetic

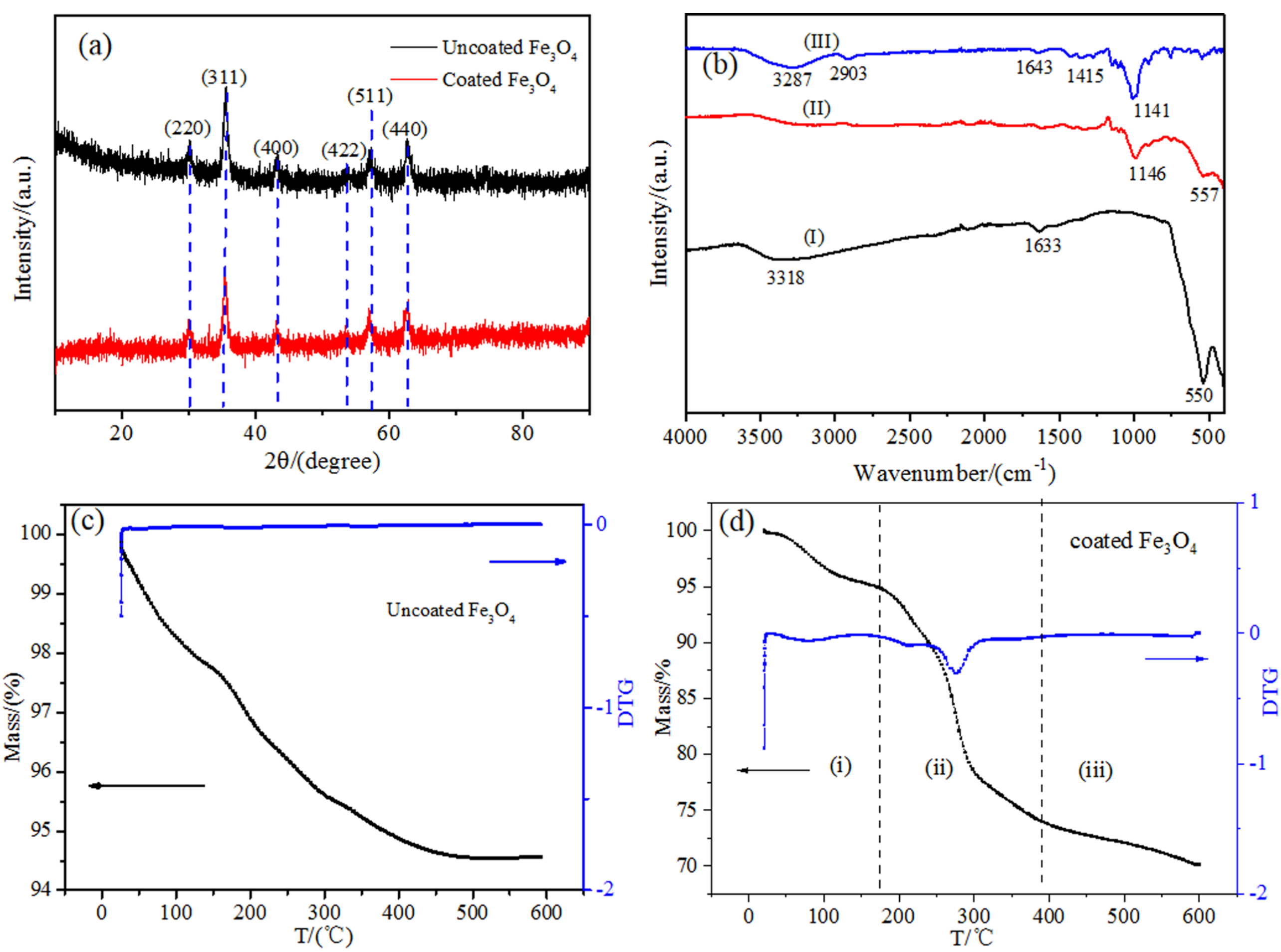

Figure 2: Characterization of MF: (a) XRD of uncoated and dextran-coated Fe_3O_4 nanoparticles; (b) FTIR of (I) uncoated Fe_3O_4 magnetic nanoparticles; (II) dextran-coated Fe_3O_4 magnetic nanoparticles; (III) dextran; (c) and (d) TG and DTG curve of uncoated and dextran-coated Fe_3O_4 magnetic nanoparticles.

nanoparticles and dextran, which indicates that the dextran has been introduced onto the surface of Fe_3O_4 magnetic nanoparticles. FTIR has successfully determined the dextran-coated magnetic nanoparticles.

Figure 2c and d exhibits thermogravimetry (TG) and differential thermogravimetry (DTG) curves of uncoated and dextran-coated Fe_3O_4 magnetic nanoparticles. From Figure 2c, the TG curve of uncoated magnetic nanoparticles looks relatively smooth. The weight loss is about 4.5%, which results from the evaporation of a small amount of water on the surface of nanoparticles. From Figure 2d, the TG curve can be divided into three stages: (i) This stage is from room temperature to 160°C, and the weight loss of the Fe_3O_4 magnetic nanoparticles is attributed to the evaporation of the water adsorbed on the surface of the particle. (ii) In the second stage (from 160 to 390°C), the weight of Fe_3O_4 magnetic nanoparticles declines sharply, and the weight loss is about 21.2%. This phenomenon is mainly due to the decomposition of dextran molecules coated on the surface of Fe_3O_4 magnetic nanoparticles. Meanwhile, it can be seen from the DTG curve that the dextran molecules have a decomposition peak at 270°C, which also proves that the dextran molecules have great thermal stability. The residues are mainly Fe_3O_4 magnetic nanoparticles. (iii) The weight loss after 390°C may attribute to the loss of oxygen-containing functions with the temperature rising [36,37]. According to the TG curve, the coating rate is about 24%. Compared to the uncoated and dextran-coated TG curve, we can conclude that the dextran has been successfully coated on the surface of magnetic nanoparticles. In conclusion, after the above characterization, we successfully prepared dextran-coated Fe_3O_4 MF.

3.2 Magnetic properties

3.2.1 Magnetic properties of Fe_3O_4 magnetic nanoparticles

The magnetic property of Fe_3O_4 magnetic nanoparticles obtained by drying the prepared MF was measured by a vibrating sample magnetometer. As shown in Figure 3a, with the increasing additional magnetic field (Oe), the magnetization intensity of the samples gradually increases until it is saturated when the additional magnetic field is large enough. The saturation magnetization (M_s) of Fe_3O_4 decreases from 66.27 to 41.02 emu/g after being modified by dextran, as the dextran coating caused the decrease in M_s. To some extent, it indirectly testifies that dextran is coupled with Fe_3O_4 magnetic nanoparticles. Nevertheless, the samples still demonstrate good magnetism. The magnetization intensity of samples rises to saturation along with the aggrandizement of the external magnetic field.

Similarly, the gradual rise in the magnetization intensity of the samples appears as the external magnetic field ascends in a reverse direction. The magnetization intensity is almost zero when there is no additional magnetic field, demonstrating that the samples exhibit superparamagnetism [38]. The remanence and the coercivity of the dextran-coated Fe_3O_4 magnetic nanoparticles are slightly

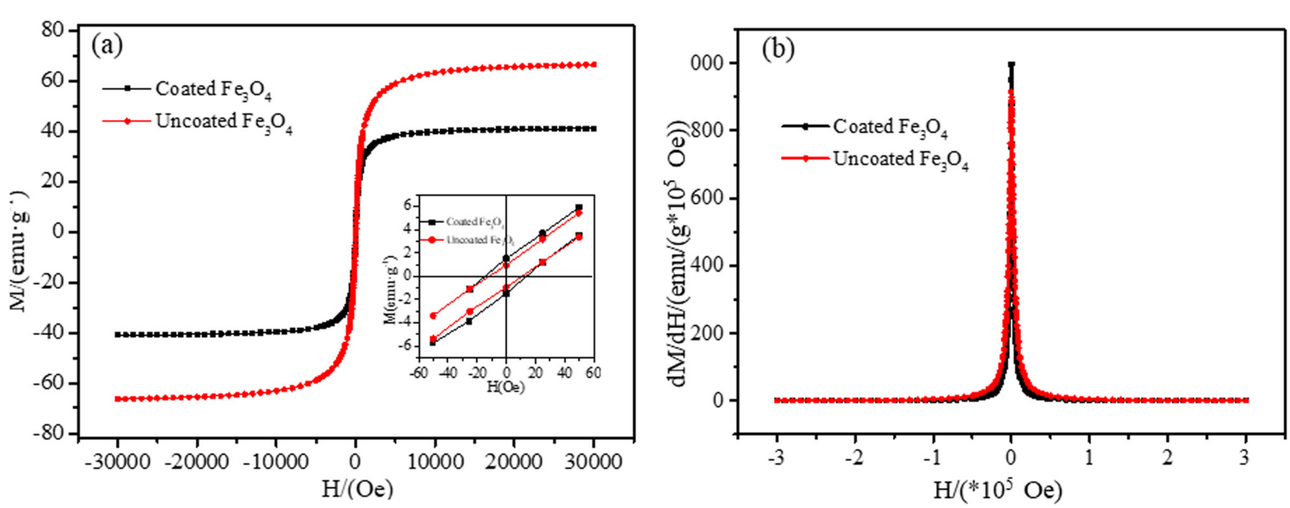

Figure 3: Hysteresis loop curves for uncoated and dextran-coated Fe_3O_4 magnetic nanoparticles (a) and corresponding susceptibility curve (b). Inset: Hysteresis loops of both samples at the low external magnetic field (a).

larger than that of the uncoated sample due to the magnetic interaction between the coated magnetic nanoparticles. Figure 3(b) shows the susceptibility (dM/dH) of the two samples, and it shows that the initial susceptibility of the dextran-coated Fe_3O_4 magnetic nanoparticles is higher than that of the uncoated Fe_3O_4 magnetic nanoparticles, because of dipolar interaction between crystals in a relatively small range of applied magnetic fields [39].

3.2.2 Magnetic property of Fe_3O_4 MF

In the low magnetic field range, the MF's susceptibility remains unchanged, which is considered a constant. In contrast, the magnetization intensity (M) of the MF is proportional to the magnetic field intensity H.

$$M = \chi H. \tag{1}$$

In a high magnetic field, the M has a tendency to be saturated, so M is M_s. M_s is a constant which can be calculated as follows:

$$f = \int_H^{H_0} (\chi - \chi_e)\mu_0 SH \frac{\partial H}{\partial z} dz, \tag{2}$$

H – magnetic intensity of magnetic field center, mT; H_0 – magnetic field intensity at the top of the sample (mT); χ – volumetric susceptibility of samples; χ_e – volumetric susceptibility of air; S – sectional area (m^2); and μ_0 – permeability of vacuum ($4\pi \times 10^{-7}$ N/A^2).

Generally, as for the MF, the value of χ_e is very small, which can be neglected. So, in the downfield, formula (2) can be simplified as follows:

$$\chi = 2f/\mu_0 SH^2. \tag{3}$$

And in a magnetic field with high intensity, the saturation magnetization can be calculated as follows:

$$M_s = f/\mu_0 SH, \tag{4}$$

$$f = (\Delta m_{s+t} - \Delta m_t)g, \tag{5}$$

$$\Delta m = m_1 - m_0, \tag{6}$$

m_1 – the weight in the magnetic field (mg); m_0 – the weight without the magnetic field (mg); m_{s+t} – the total weight of the MF and the glass tube (mg); and m_t – the weight of the glass tube (mg).

Increased magnetic gravity f in different magnetic fields, the intensity H is gained by the measurement of Gouy magnetic balance. Then, the relationship curve between the increased magnetic weights and magnetic field intensity can be drawn as shown in Figure 4. The magnetic susceptibility χ and saturation magnetization M_s of water-based MF can be obtained based on the formulas (3) and (4). The values are $\chi = 5.87 \times 10^{-4}$, M_s = 20.57 emu/g. As a result, it is not difficult to see that the magnetic susceptibility and the saturation magnetization of the prepared dextran-coated Fe_3O_4 MF are high [40].

Combined with the above data, we can conclude that the magnetic properties of nanoparticles decreased significantly, which is due to the coating of dextran [24]; however, the magnetic properties of MF are excellent because the dextran-coated ferric oxide can fully ensure the hydrophilicity of MF. In addition, after centrifugation, the excess dextran is separated, so the coating rate is about 24% by TG, which further improves the magnetic property.

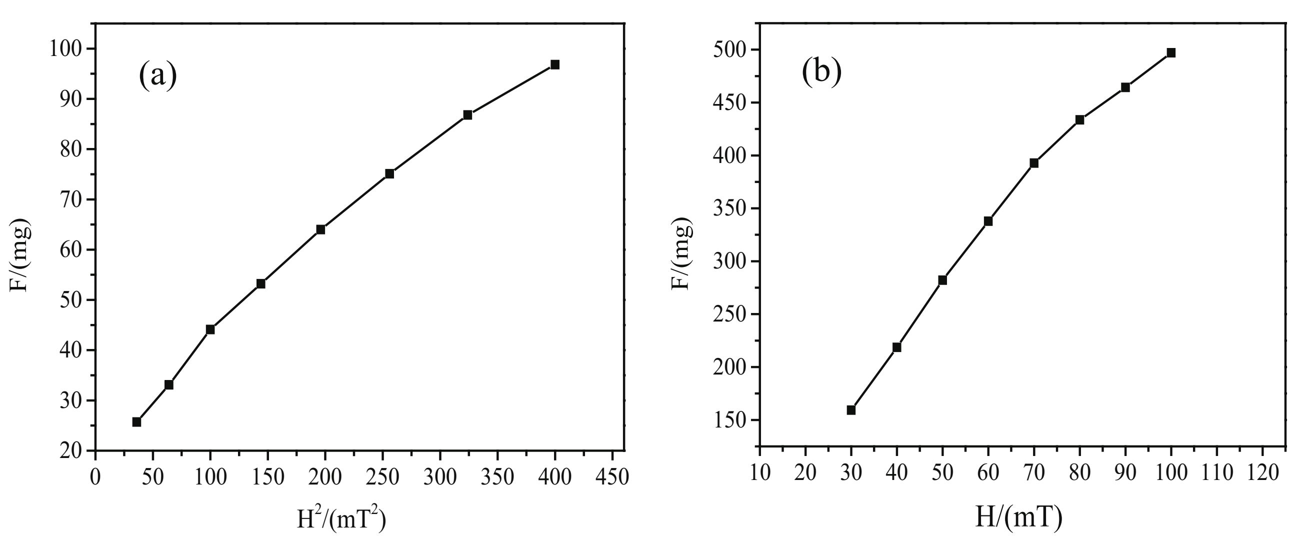

Figure 4: Relationship between the magnetic weight of MF and magnetic field intensity, corresponding to (a) F–H^2 curve and (b) F–H curve.

3.3 Stability of MF

Excellent stability is the prerequisite for the effective application of MF. The stability of the prepared MF is discussed by using magnetic field stability, dilution stability, and autoclaved stability.

The stability of MF under a gravity field is expressed by stability index (I) and detected by Gouy magnetic balance, I show as follows [41]:

$$I = (\rho_1 - \rho_w)/(\rho - \rho_w),$$

ρ_1 – the density of the upper layer of the MF after a period of time (g/cm^3); ρ – the density of the fresh MF (g/cm^3); and ρ_w – the density of deionized water (g/cm^3).

The density of the upper layer of the MF and fresh MF is tested, and I curves of the samples after standing for different times are shown in Figure 5a. As revealed in Figure 5a, there will be a small amount of precipitation in the first few days. After that, I stays almost unchanged. That is to say, the Fe_3O_4 MF is relatively stable, and almost no precipitate is generated. In total, the prepared MF has favorable stability.

The magnetic stability of MF is certified by the change in the magnetic weight, which is tested for 6 h by Gouy magnetic balance in stable magnetic field intensity. From Figure 5b, it can be observed that the magnetic weight almost stays unchanged with the prolonging of time in 25 mT. That is to say, the MF owns the ability to keep the monodispersity in a magnetic field, exhibiting outstanding magnetic stability.

The MF will be greatly diluted after the injection into the human body; meanwhile, the dilution stability of the MF must be investigated for practical application. The sample was diluted with deionized water at the ratio of

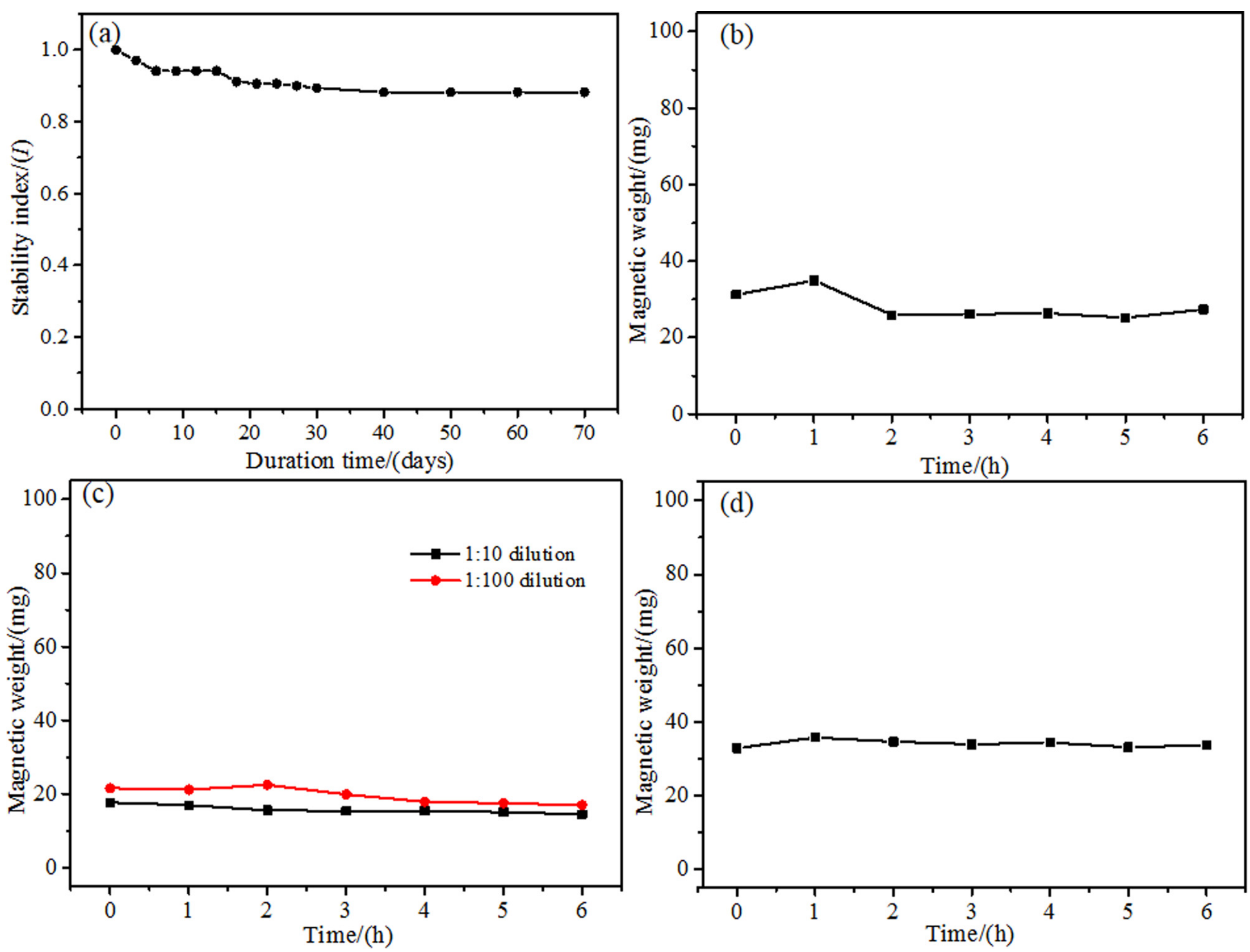

Figure 5: Stability of MF: (a) change in stability index of the MF *vs* duration time; (b) relationship between the increased magnetic weight of MF and time in a magnetic field intensity of 25 mT; (c) the relationship between the increased magnetic weight of diluted MF and time in a magnetic field intensity of 25 mT; and (d) the relationship between the increased magnetic weight of autoclaved MF and time a in magnetic field intensity of 25 mT.

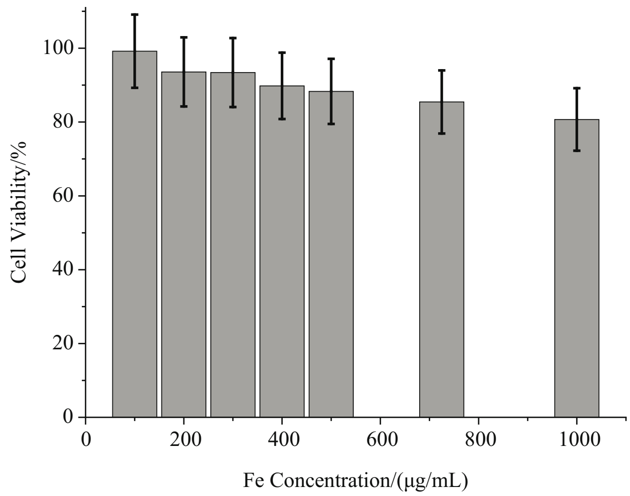

Figure 6: Viability of MCF-7 cells after incubation with dextran-coated MF with different concentrations of Fe for 24 h.

1:10 and 1:100, and the stability was measured by Gouy magnetic balance in a constant magnetic field (H = 25 mT). The magnetic stability of the samples was determined like the process of magnetic weight gain stability. As shown in Figure 5c, the magnetic weight of both 10 times and 100 times diluted MF are almost constant. It indicates that the MF exhibits great magnetic stability after being diluted.

The MF must be nontoxic for *in vivo* biomedical applications. So, the MF must exhibit superb stability after being autoclaved. After being autoclaved, the magnetic stability of the MF is investigated. The MF was sterilized in a high-pressure steam sterilizer at 120°C for 10 min. From Figure 5d, it can be seen clearly that the magnetic weight of the autoclaved MF can keep stable in the magnetic field of 25 mT.

Through the above research, it is fully proved that the MF has excellent stability. This is mainly because dextran is added several times during the preparation of MF, which ensures that the iron oxide in the core is fully coated, to ensure excellent water solubility and stability.

3.4 Toxicological experiments

3.4.1 *In vitro* toxicity

Figure 6 shows the survival rate of MCF-7 cells after being incubated with dextran-coated Fe_3O_4 MF in different iron concentrations (0–1,000 μg/mL of Fe) for 24 h. It can be seen that when the Fe concentration was low at 100 μg/mL, the cell viability exceeds 100% after being cultivated with the MF for 24 h. Meanwhile, the higher the concentration, the lower the cell viability, even when the iron concentration is as high as 700 μg/mL, the cell survival rate remains about 85%, which indicates that the prepared dextran-coated water-based MF is extremely low cell cytotoxicity for MCF-7 cells.

3.4.2 *In vivo* toxicity

To further study the biocompatibility of the prepared MF, we used short-term and long-term distribution experiments to study the *in vivo* toxicity of mice with different doses. The changes in leukocyte count and acute toxicity were counted and studied, the details are as follows.

3.4.2.1 Effect of MF on peripheral blood system in mice

None of the mice died during the experiments. The total number of white blood cells was not statistically significant ($p > 0.05$) [42] compared with the control group after 12, 24, and 36 h of vein injection. The results show that the lethal median dose was more than 1,136 mg/kg (LD50 > 1,136 mg/kg), the maximum nontoxic dose (ED0) was 652 mg/kg, the LD50 was more than 2,166 mg/kg, and the ED0 was 1,338 mg/kg for intraperitoneal administration, which suggested that Fe_3O_4 MF was nontoxic, as shown in Table 1.

Table 1: Number of white blood cells after different doses of injection

Groups (n = 5)	Dose of the MF (mg/kg)	Before giving MF ($\times 10^9$/L)	12 h after giving MF ($\times 10^9$/L)	24 h after giving MF ($\times 10^9$/L)	36 h after giving MF ($\times 10^9$/L)
Control group	—	7.2 ± 1.8	7.3 ± 2.5	7.3 ± 2.0	7.1 ± 2.8
Low dose group	652	7.3 ± 2.2	7.3 ± 2.1	7.5 ± 2.2	7.3 ± 2.0
Middle dose group	909	7.2 ± 2.1	7.3 ± 2.4	7.5 ± 2.1	7.4 ± 2.2
High dose group	1,136	7.2 ± 2.2	7.5 ± 2.5	7.5 ± 2.0	7.5 ± 2.6

Note: Comparing between groups, the F values were 0.63, 0.65, and 0.63, and the P values were 0.61, 0.60, and 0.61, after 12, 24, and 36 h of MF injection, respectively.

Table 2: Results of MF after intravenous injection

Groups (n = 5)	Dose of MF (mg/kg)	Weight before giving MF(g)	Weight after 10 days of MF injection (g)	Observation index				Death situation
				Appetite	Diarrhea	Somnolence	Activity	
Control group	—	22.4 ± 0.9	22.4 ± 0.9	Good	None	None	Normal	None
Low dose group	652	23.4 ± 0.9	23.4 ± 0.9	Good	None	None	Normal	None
Middle dose group	909	22.1 ± 0.8	22.2 ± 0.8	Poorer	None	None	Normal	None
High dose group	1,136	22.7 ± 0.9	22.7 ± 0.9	Poorer	None	Having	Slightly worse	None

Note: In comparison between groups, F value was 0.31, and P value was 0.59 after 10 days of MF injection.

Table 3: Results of MF after intraperitoneal injection

Groups (n = 5)	Dose of MF (mg/kg)	Weight before giving MF (g)	Weight after 10 days of MF injection (g)	Observation index				Death situation
				Appetite	Diarrhea	Somnolence	Activity	
Control group	—	23.1 ± 0.9	37.3 ± 1.4	Good	None	None	Normal	None
Low dose group	1,338	22.4 ± 0.9	36.8 ± 1.3	Good	None	None	Normal	None
Middle dose group	1,757	22.8 ± 0.9	37.0 ± 1.3	Poorer	None	None	Normal	None
High dose group	2,163	23.1 ± 0.9	38.4 ± 1.6	Poorer	None	Having	Slightly worse	None

Note: In comparison between groups, F value was 0.31, and P value was 0.59 after 10 days of MF injection.

3.4.2.2 Vein injection method

None of the mice died during the experiments. If the concentration of MF is further increased, there will be excess MF flowing down the injection port. The tail vein injection at 1,136 mg/kg was the largest dose of intravenous delivery in mice. Therefore, according to the recommendations of the Center for Drug Evaluation and Research of the US Food and Drug Administration for single-dose acute toxicity testing, the mice had a half-lethal dose (LD50) >1,136 mg/kg. The maximum nontoxic dose of ED0 was 652 mg/kg. There was no significant difference in body weight between the three doses and control groups ($p > 0.05$). The results are exhibited in Table 2.

3.4.2.3 Intraperitoneal injection method

The mice were intraperitoneally injected with the highest dose and the maximum drug volume, and no death was caused. The maximum tolerated dose (MTD) of mice was measured by intraperitoneally injecting based on the guidelines of toxicology research formulated by the Ministry of Health of the People's Republic of China in 2003. The performance of the mice was observed for 10 days after injecting Fe_3O_4 MF with a solid content of 2,162 mg/kg intraperitoneally. After administration, some mice developed a poor appetite and returned to normal on the second day. No mice died during the observation period. The intraperitoneal injection of MTD = 2,162 mg/kg, LD50 >2,162 mg/kg, and ED0 was 1,338 mg/kg. The body weight after administration in the three-dose groups was compared with the control group ($p > 0.05$). The results are shown in Table 3.

In summary, no matter the high-dose administration or the change in administration mode, there was no obvious toxic change in blood compatibility and subjective signs, and the value of ED0 and LD50 was large, so it suggests that the MF is safe for biological application. The reason for such excellent biocompatibility is the sufficient coating of ferric oxide by dextran.

3.5 Hyperthermia of MF

3.5.1 Hyperthermia of MF in a standard cuvette

MF can be used for the hyperthermia treatment of the tumor under an alternating magnetic field, and the temperature used for the treatment should be a minimum of 42°C [23]. This section measured the exothermic ability of the MF with three concentrations in an alternating magnetic field generated by an AC magnetic field generator using an alcohol thermometer. The frequency applied in the present investigation was 60 kHz. The experimental setup was shown in our published article [43].

From Figure 7, it can be seen that the temperature of the three concentrations of MFs in a circuit with an alternating electrical current of 11 A rises gradually. The temperature of sample rises to 51°C from 11°C in 800 s, whereas the temperature of samples b and c rises by 25 and 10°C, respectively. The weight concentration of samples a, b, and c are 55, 35, and 25 mg/mL, respectively. However, as time went on, the temperature of the MF reached a plateau. The reason is that the generated heat is equal to the amount of heat emitted to the environment, so the temperature would not rise anymore as time elapsed. Moreover, the temperature is controlled by the Curie temperature of the Fe_3O_4 magnetic nanoparticles. So the temperature rises enough to kill cancer cells around the tissue [25].

3.5.2 Hyperthermia of human lung cancer A549 cells

Meanwhile, the obtained MF exhibits great potential in the application in MF hyperthermia of tumors. In this section, an AC magnetic field generator measured the effect of Fe_3O_4 MF hyperthermia on the human lung cancer A549 cell line *in vitro*. The MF and lung cancer A549 cells were co-cultured and heated in an alternating magnetic field, which could be elevated to above 42°C. The morphological changes in human lung cancer cells in each group after hyperthermia (×800) were exhibited. One of them was the control group (Figure 8a), the cell size was the same, no cell rupture, and the growth was

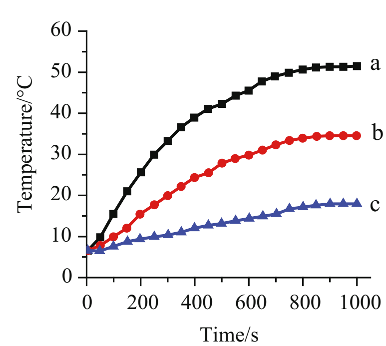

Figure 7: Heating curves of dextran-coated Fe_3O_4 magnetic nanoparticles with different concentrations (25, 35, and 55 mg/mL) at fixed apparent current ($I = 300$ A), a is 55 mg/mL, b is 35 mg/mL, c is 25 mg/mL.

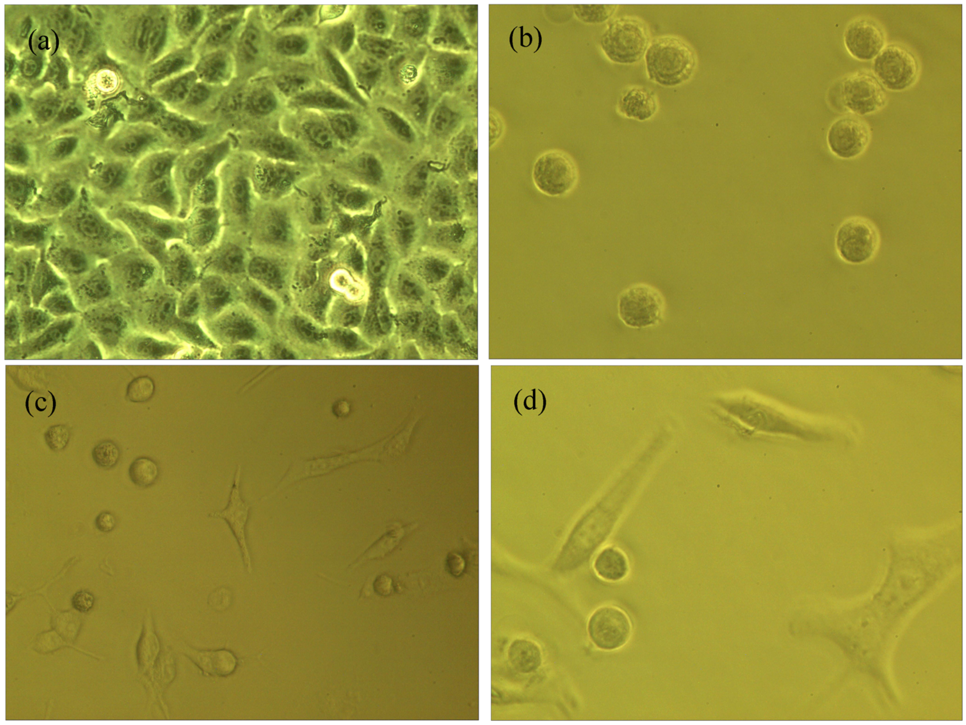

Figure 8: The morphology of human lung cancer A549 cell line in the light microscope (×800) after the MF hyperthermia: (a) control group and (b)–(d) experimental group with 55 mg/mL at 300 A.

strong. In addition, Figure 8(b–d) were the experimental groups, in which it can be seen that the number of lung cancer cells was gradually reduced after hyperthermia of lung cancer cells, while necrotic cells and cell debris were gradually increased. In conclusion, dextran-coated MF shows certain magnetic hyperthermia abilities.

In short, the biological properties of MF were significantly improved due to the addition of dextran. In addition, dextran is added several times in the preparation process, which makes dextran fully coordinated with ferric oxide, to prepare MF with excellent stability. Therefore, it shows a certain application potential in hyperthermia.

4 Conclusion

Dextran-coated Fe_3O_4 MF was successfully prepared by chemical co-precipitation. MF shows excellent stability, which is embodied in magnetic stability, dilution stability, and autoclaved stability. Meanwhile, the M_s and susceptibility are very high while the coercivity and remanence of the obtained MF are very small, which can be considered superparamagnetism. In addition, the biological toxicity *in vivo* and *in vitro* showed that dextran-coated Fe_3O_4 MF had excellent biocompatibility, so it exhibits great potential for biological applications. So, when applied to lung cancer A549 cells, it can quickly and effectively kill cancer cells, showing a certain application potential. Of course, the research on MF preparation needs to go on if we expect to obtain more MF with outstanding properties, which can be considered a promising development direction.

Funding information: This research was gratefully acknowledged by the financial support from the National Natural Science Foundation of China (NSFC) (No. 21246002), Minjiang Scholarship of Fujian Province (No. Min-Gaojiao [2010]-117), Central-government Guided Fund for Local Economic Development (No. 830170778), R&D Fund for Strategic Emerging Industry of Fujian Province (No. 82918001), International Cooperation Project of Fujian Science and Technology Department (No. 830170771), Open Fund of Fujian Key Laboratory of New Energy Generation and Power Conversion (No. KLIF-202102) and Analytical Testing Fund of Qingyuan Innovation Laboratory of Fujian Province.

Author contributions: All authors have accepted responsibility for the entire content of this manuscript and approved its submission.

Conflict of interest: The authors state no conflict of interest.

Ethical approval: The research related to animals' use has been complied with all the relevant national regulations and institutional policies for the care and use of animals.

References

[1] Khabarov YG, Veshnyakov V, Komarova G, Kuzyakov N, Chukhchin D. Using nitrated lignosulfonates for the synthesis of a water-based magnetic fluid. Int J Nanosci. 2019;18(2):1850018.
[2] Fu LP, Ma QL, Liao KL, An JN, Bai JM, He YF. Application of Pickering emulsion in oil drilling. Nanotechnol Rev. 2022;11:26–39.
[3] Bagheli S, Fadafan HK, Orimi RL, Ghaemi M. Synthesis and experimental investigation of the electrical conductivity of water based magnetite nanofluids. Powder Technol. 2015;274:426–30.
[4] Manuzzo R, Califano F, Belmont G, Rezeau L. A multi-fluid model of the magnetopause. Ann Geophys. 2020;38:275–86.
[5] Lima G, Nalon GH, Santos RF, Ribeiro JCL, Araújo END. Microstructural investigation of the effects of carbon black nanoparticles on hydration mechanisms, mechanical and piezoresistive properties of cement mortars. Mater Re. 2021;24(4):e20200539.
[6] Li HC, Yang SQ, David H, Hong RY. Progress in magnetic Fe_3O_4 nanomaterials in magnetic resonance imaging. Nanotechnol Rev. 2020;9:1265–83.
[7] Wu K, Su DQ, Saha R, Wong D, Wang JP. Magnetic particle spectroscopy-based bioassays: methods, applications, advances, and future opportunities. J Phys D Appl Phys. 2019;52(17):173001.
[8] Pawlik P, Blasiak B, Depciuch J, Pruba M, Kitala D, Vorobyova S, et al. Application of iron-based magnetic nanoparticles stabilized with triethanolammonium oleate for theranostics. J Mater Sci. 2022;57:4716–37.
[9] Bullivant JP, Zhao S, Willenberg BJ, Kozissnik B, Batich CD, Dobson J. Materials characterization of feraheme/ferumoxytol and preliminary evaluation of its potential for magnetic fluid hyperthermia. Int J Mol Sci. 2013;14:17501–10.
[10] Alberto N, Domingues MF, Marques C, André P, Antunes P. Optical fiber magnetic field sensors based on magnetic fluid: a review. Sensors. 2018;18(12):4325.
[11] Kabe Y, Sakamoto S, Hatakeyama M, Yamaguchi Y, Suematsu M, Itonaga M, et al. Application of high-performance magnetic nanobeads to biological sensing devices. Anal Bioanal Chem. 2019;411(9):1825–37.
[12] Qiu J, Luo YP, Li YQ, Luo J, Su ZB, Wang Y. Research on a mechanical model of magnetorheological fluid different diameter particles. Nanotechnol Rev. 2020;11(1):158–66.
[13] Correia DM, Sencadas V, Ribeiro C, Martins PM, Martins P, Gama FM. Processing and size range separation of pristine and magnetic poly(L-lactic acid) based microspheres for biomedical applications. J Colloid Interf Sci. 2016;476:79–86.
[14] Maffei ME. Magnetic fields and cancer: epidemiology, cellular biology, and theranostics. Int J Mol Sci. 2022;23(3):1339.
[15] Racuciu M, Oancea S. Characterization of the oxidation of magnetite nanoparticles during their synthesis by different structural analysis techniques. Anal Lett. 2020;54(1–2):173–83.
[16] Goharkhah M, Ashjaee M, Shahabadi M. Experimental investigation on convective heat transfer and hydrodynamic characteristics of magnetite nanofluid under the influence of an alternating magnetic field. Int Therm Sci. 2016;99:113–24.
[17] Ebadi M, Bullo S, Buskaran K, Hussein Mohd HZ, Fakurazi S, Pastorin G. Dual-functional iron oxide nanoparticles coated with polyvinyl alcohol/5-fluorouracil/zinc-aluminium-layered double hydroxide for a simultaneous drug and target delivery system. Polymers. 2021;13(6):855.
[18] Rahman MA, Ochiai B. Fabrication and hemocompatibility of carboxy-chitosan stabilized magnetite nanoparticles. Microsyst Technol. 2017;24(1):669–81.
[19] Thi Thu HL, Thuc QB, Thi Minh TH, Le MH, Hong NP, Phuong TH. Optimizing the alginate coating layer of doxorubicin-loaded iron oxide nanoparticles for cancer hyperthermia and chemotherapy. J Mater Sci. 2018;53:13826–42.
[20] Craciunescu I, Chiţanu E, Codescu MM, Iacob N, Kuncser A, Kuncser V, et al. High performance magnetorheological fluids: very high magnetization FeCo-Fe_3O_4 nanoclusters in a ferrofluid carrier. Soft Mater. 2022;18(3):626–39.
[21] Arefyev IM, Demidenko OV, Saikin MS. Assessment of magnetic fluid stability in non-homogeneous magnetic field of a single-tooth magnetic fluid sealer. J Magn Magn Mater. 2017;431:20–3.
[22] Sakaguchi M, Makino M, Ohura T, Yamamoto K, Enomoto Y, Takase H. Surface modification of Fe_3O_4 nanoparticles with dextran *via* a coupling reaction between naked Fe_3O_4 mechano-cation and naked dextran mechano-anion: a new mechanism of covalent bond formation. Adv Power Technol. 2019;30(4):795–806.
[23] Liu G, Hong RY, Guo L, Liu GH, Feng B, Li YG. Exothermic effect of dextran-coated Fe_3O_4 magnetic fluid and its compatibility with blood. Colloids Surf A: Physicochem Eng Asp. 2011;380:327–33.
[24] Shaterabadia Z, Nabiyounia G, Soleymani M. Correlation between effects of the particle size and magnetic field strength on the magnetic hyperthermia efficiency of dextran-coated magnetite nanoparticles. Mat Sci Eng C-Mater. 2020;117:111274.
[25] Linh PH, Phuc NX, Hong LV, Uyen LL, Chien NV, Nam PH, et al. Dextran coated magnetite high susceptibility nanoparticles for hyperthermia applications. J Magn Magn Mater. 2018;460(15):128–36.
[26] Nemala H, Thakur JS, Naik VM, Vaishnava PP, Lawes G, Naik R. Investigation of magnetic properties of Fe_3O_4 nanoparticles using temperature dependent magnetic hyperthermia in ferrofluids. J Appl Phys. 2014;116:034309.
[27] Lee H, Son YS, Lee MO, Ryu JW, Park K, Kwon O, et al. Low-dose interleukin-2 alleviates dextran sodium sulfate-induced colitis in mice by recovering intestinal integrity and inhibiting AKT-dependent pathways. Theranostics. 2020;10(11):5048–63.
[28] Strbak O, Antal I, Khmara I, Koneracka M, Kubovcikova M, Zavisova V, et al. Influence of dextran molecular weight on the physical properties of magnetic nanoparticles for hyperthermia and MRI applications. Nanomaterials. 2020;10:2468.
[29] Shirvalilou S, Khoei S, Khoee S, Raoufi NJ, Karimi MR, Shakeri-Zadeh A. Development of a magnetic nano-graphene oxide carrier for improved glioma-targeted drug delivery and

imaging: *in vitro* and *in vivo* evaluations. Chem-Bio Interact. 2018;295:97–108.
[30] Wong BT, Day L, Augustin MA. Deamidated wheat protein-dextran Maillard conjugates: effect of size and location of polysaccharide conjugated on steric stabilization of emulsions at acidic pH. Food Hydrocolloid. 2011;25(6):424–1432.
[31] Karnati SR, Oldham D, Fini EH, Zhang LF. Surface functionalization of silica nanoparticles to enhance aging resistance of asphalt binder. Constr Build Mater. 2019;211:1065–72.
[32] Shu R, Wang M, Yang Y, Chang S, Zhang G, Gan Y, et al. Solvothermal synthesis of reduced graphene oxide/ferroferric oxide hybrid composites with enhanced microwave absorption properties. Nano. 2017;12(12):21–33.
[33] Roy S, Ghosh MP, Mukherjee S. Introducing magnetic properties in Fe-doped ZnO nanoparticles. Appl Phys A-Mater. 2021;127(6):451.
[34] Khatik R, Wang ZY, Li FF, Zhi D, Yang Q. “Magnus nano-bullets” as T-1/T-2 based dual-modal for *in vitro* and *in vivo* MRI visualization. Nanomed-Nanotechnol. 2019;15:264–73.
[35] Wang ZZ, Ji LY, Ren YM, Liu MH, Ai XY, Yan C. Preparation and anti-tumor study of dextran 70,000-selenium nanoparticles and poloxamer 188-selenium nanoparticles. AAPS PharmSciTech. 2022;23:29.
[36] He L, Zheng R, Min J, Su H. Preparation of magnetic microgels based on dextran for stimuli-responsive release of doxorubicin. J Magn Magn Mater. 2021;517:167394.
[37] Castillejos E, Esteban-Arranz A, Bachiller-Baeza B, Rodriguez-Ramos I, Guerrero-Ruiz A. Reductive degradation of 2,4-dichlorophenoxyacetic acid using Pd/carbon with bifunctional mechanism. Catal Today. 2020;357:361–7.
[38] Lou PC, Laura D, Tang C, Alex G, Sandeep K. Spin phonon interactions and magneto-thermal transport behavior in p-Si. Solid State Commun. 2018;283:37–42.
[39] Linh PH, Phuc NX, Hong LV, Uyen LL, Chien NV, Nam PH, et al. Dextran coated magnetite high susceptibility nanoparticles for hyperthermia applications. J Magn Magn Mater. 2021;460:128–36.
[40] Jin S, Park BC, Ham WS, Pan L, Kim YK. Effect of the magnetic core size of amino-functionalized Fe_3O_4-mesoporous SiO_2 core-shell nanoparticles on the removal of heavy metal ions. Collid Surf A. 2017;531:133–40.
[41] Li HC, Li TH, Wu Q, Wang R, Hong RY. Super stable water-based magnetic fluid as a dual-mode contrast agent. Nanotechnol Rev. 2021;10(1):1031–45.
[42] Köhler O, Sylvia LG, Bowden CL, Calabrese JR, Thase M, Shelton RC, et al. White blood cell count correlates with mood symptom severity and specific mood symptoms in bipolar disorder. Aust Nz J Psychiat. 2017;51(4):355–65.
[43] Xu D, Tang WJ, Zhu YZ, Liu Z, Yang K, Liang MX, et al. Hyperthermia promotes exosome secretion by regulating Rab7b while increasing drug sensitivity in adriamycin-resistant breast cancer. Int J Hyperther. 2022;39(1):246–57.